



CHORUS

This is the accepted manuscript made available via CHORUS. The article has been published as:

Room Temperature Ultralow Threshold GaN Nanowire Polariton Laser

Ayan Das, Junseok Heo, Marc Jankowski, Wei Guo, Lei Zhang, Hui Deng, and Pallab
Bhattacharya

Phys. Rev. Lett. **107**, 066405 — Published 4 August 2011

DOI: [10.1103/PhysRevLett.107.066405](https://doi.org/10.1103/PhysRevLett.107.066405)

A Room Temperature Ultra-Low Threshold GaN Nanowire-Polariton Laser

Ayan Das¹, Junseok Heo¹, Marc Jankowski¹, Wei Guo¹, Lei Zhang², Hui Deng²
and Pallab Bhattacharya^{1,*}

¹*Center for Nanoscale Photonics and Spintronics, Department of Electrical Engineering and Computer Science, University of Michigan, Ann Arbor, Michigan 48109, USA*

²*Department of Physics, University of Michigan, Ann Arbor, Michigan 48109, USA*

Abstract

We report ultra-low threshold polariton lasing from a single GaN nanowire strongly-coupled to a large-area dielectric microcavity. The threshold carrier density is three orders of magnitude lower than that of photon-lasing observed in the same device, and two orders of magnitude lower than any existing room-temperature polariton devices. Spectral, polarization, and coherence properties of the emission were measured to confirm polariton lasing.

* Email: pkb@eecs.umich.edu

Strong-coupling effects¹⁻³ and polariton lasing⁴⁻⁷ are currently subjects of intense research. Polariton lasing was reported in GaAs-quantum well (QW) microcavities at a threshold density two orders of magnitude lower than that of photon lasing in the same device^{5,8}. GaAs-based polariton systems, however, do not survive at higher temperatures due to the small exciton binding energy and exciton-photon interaction energy of ~ 10 meV. Candidates for room temperature polariton lasers include systems using III-N^{6,9}, ZnSe¹⁰, ZnO¹¹, or organic molecules¹² as the electronic media. Polariton lasing at room temperature was reported in bulk organic microcavities⁷, and in bulk⁶ and multiple-quantum-well (QW)¹³ GaN microcavities. However, the threshold density in organic cavities is still higher than some competing lasing mechanisms in the device, and in III-nitride microcavities, only modest improvement was obtained compared to weakly-coupled GaN QW devices. Furthermore, in III-nitride bulk-microcavity and QW-microcavity structures the media and photon coupling is significantly reduced by a large built-in polarization field¹⁴; the optical quality and reproducibility of the devices are often compromised by relatively large compositional inhomogeneities and structural defects¹⁵.

In this work, we developed a new structure — GaN nanowires — as the active media, and produced a room-temperature polariton laser operating at an energy threshold orders of magnitude lower than before. Remarkably, the nanowires are free of extended defects, have no alloy fluctuation to introduce inhomogeneous broadening, have a surface recombination velocity $\sim 10^3$ cm/s, which is two orders of magnitude smaller than that of GaAs, and very small surface depletion and thus are easily reproducible¹⁶⁻²⁰. It has been seen experimentally that the polarization field in the nanowires is negligible²¹ and the internal quantum efficiency is $\sim 50-60\%$. We enclosed a single nanowire in a dielectric microcavity. The characteristic polariton dispersions were measured by angle-resolved photoluminescence. We also studied the linewidth narrowing and energy shift of the lasing mode, population redistribution in the momentum space,

and coherence functions of the polariton laser. A second threshold, which we believe corresponds to photon lasing with an inverted carrier population, was observed at 2700 times the polariton lasing threshold.

The GaN nanowire-microcavity used in this study is shown schematically in Fig. 1(a). It consists of a SiO_2 λ -cavity sandwiched by a top and a bottom distributed Bragg reflector (DBR) made of 7 pairs of $\text{SiO}_2/\text{TiO}_2$. A single nanowire is placed at the central antinode of the cavity field to maximize the interaction between the GaN nanowire excitons and the cavity mode. The inset to Fig. 1(a) shows the scanning electron microscope image of the nanowire lying on the half cavity, before the top cavity was deposited. The wire has a diameter of ~ 60 nm and a length of ~ 750 nm. The nanowire diameter corresponds to the total thickness of 50 quantum wells used in similar devices¹³. A low background carrier concentration of $8.5 \times 10^{16} \text{ cm}^{-3}$ was derived from measurements made on Pt-GaN nanowire Schottky diodes¹⁷. A photoluminescence (PL) spectrum of the nanowires at 25 K is shown in Fig 1(b). The three free exciton transitions, $X_{A,B,C}$, corresponding to the wurtzite crystalline structure are indicated. The peaks labelled DBX_A and DBX_B are bound exciton transitions. The broad and weak transition at ~ 3.41 eV is related to the surface¹⁷. The lineshape of the exciton transitions resembles a Lorentzian function instead of a Gaussian function, suggesting negligible inhomogeneous broadening of the exciton resonances in the nanowires. After the complete cavity is fabricated, enclosing the nanowire, the cavity is etched into a mesa of $5 \mu\text{m}$ diameter (see supplementary document). We have studied two devices, fabricated from different samples of GaN nanowires with different cavity-exciton detunings. The measured results are qualitatively similar and in the following we describe the sample which is negatively detuned at 300K.

We measured the dispersion of the resonant modes at 300 K by angle-resolved photoluminescence and the spectra are shown in Fig. 1(c). A peak below the exciton resonances

is clearly observed in the spectra, which asymptotically approaches the X_A exciton energy at larger angles. A weaker peak above the exciton resonances can also be identified, and the two peaks anti-cross with increasing angle. Using the one-to-one correspondence between the angle of the out-coupled photon and the in-plane wavenumber of the polaritons, we obtained the energy-momentum dispersion of the resonances (Fig. 1(d)). The results are well described by the polariton dispersions calculated by the coupled oscillator model (as shown by the solid curves). Here we consider only coupling of X_A exciton and the cavity mode, because the X_B and X_C excitons have much weaker oscillator strengths according to PL measurements. The cavity to exciton detuning δ and photon-exciton interaction potential V_A are obtained by fitting the data and are found to be $\delta = -20$ meV and $V_A = 48$ meV for the X_A exciton. The exciton linewidth without thermal broadening used in the Hamiltonian is $\Gamma_{X_A} = 4.5$ meV and is obtained from independent photoluminescence measurement on a single GaN nanowire at 25 K. The relatively large value of V_A for a single nanowire is due to both the large oscillator strength of excitons resulting from a small internal electric field of ~ 0.19 MV/cm^{20,21}, and a modified cavity field that concentrates within the nanowire. Since the refractive index of the nanowire is higher than that of the cavity, the cavity field is mainly within the nanowire region even without additional transverse confinement of the cavity mode. This is confirmed by finite difference time domain (FDTD) simulations (see supplementary document). The polarization field in a bulk GaN microcavity is calculated to be ~ 1 MV/cm for a reported compressive stress of 30 kBar¹⁰. The oscillator strength in the single nanowire is therefore approximately twice than in the bulk microcavity²² and the interaction potential V_A is expected to be ~ 44 meV compared to the bulk value of 31 meV¹⁰. Consistent polariton dispersions similar to the data of Fig. 2 were also obtained at 200K (see supplementary document).

To investigate the non-linear optical properties of the nanowire microcavities, we pump the device non-resonantly with a frequency-tripled Ti-Sapphire laser focused to a spot size of $\sim 100\mu\text{m}$ in diameter. Photoluminescence from the normal direction was analyzed with a high resolution monochromator (with a spectral resolution of $\sim 0.03\text{ nm}$), and detected with a photomultiplier tube using phase-sensitive lock-in amplification. With increasing pumping power, a sharp super-linear increase of the PL intensity from lower polaritons (LPs) at $k_{\parallel}\sim 0$ was observed at both 200 and 300K (Fig. 2), accompanied by a sharp decrease in the emission linewidth and a small blueshift of the LP energy. Both features indicate the onset of stimulated scattering into the LP states near $k_{\parallel}=0$. The incident excitation energy at threshold was $E_{\text{th1}} = 92.5\text{ nJ/cm}^2$ at 300 K and 63 nJ/cm^2 at 200 K. We estimate an upper bound of the LP density at the threshold to be $N_{\text{LP}}(E_{\text{th1}}) = 2 \times 10^{16}\text{ cm}^{-3}$, using the relation $N_{3\text{D}} < E_{\text{th1}}/(E_{\text{pump}}D)$. The LP density at the threshold, $N_{\text{LP}}(E_{\text{th1}})$, is two orders of magnitude lower than any previously reported GaN polariton lasers, and three orders of magnitude less than the exciton Mott density of $3 \times 10^{19}\text{ cm}^{-3}$,²³ the latter corresponding to the required carrier density for conventional photon lasing. Remarkably, the gain media in our device is a single nanowire with the lateral size of $\sim 0.045\mu\text{m}^2$, which is orders of magnitude smaller than the optical excitation spot size used in these measurements. Therefore the nanowire-microcavity device can allow further reduction in the threshold energy with electrical injection.

Above threshold, the emission spectra showed multiple peaks with greatly reduced linewidths, corresponding to different transverse modes of the LPs due to localization of the LP modes by the nanowires. Similar multi-mode lasing has been observed in bulk⁶ and multiple-QW¹³ GaN microcavities, where the localization was attributed to photonic disorders in the structures, and the modes varied with spatial alignment of the pump with the sample. In contrast, in our device,

the modes are intrinsic to the nanowire-microcavity. They are not due to crystal defects and do not depend on the spatial alignment of the pump. Below threshold, the modes are indistinguishable due to a thermally broadened linewidth of >10 meV. At threshold, the linewidths are greatly reduced to a mere 0.67 meV at 200K and 1.1 meV at 300K, and thus revealing the discrete modes in the spectra. The reduction in linewidth indicates the increase in the coherence time of the LPs in the lasing mode to 6.2 ps at 200K and 3.8 ps at 300K. Identical polariton lasing characteristics were observed for the second device (shown in supplementary document).

A small blueshift δE of the LP emission was observed with increasing pump power up to $\delta E \sim 1.78$ meV (200K) and 1.92 meV (300K) around the threshold. Further increasing excitation density above threshold led to only negligible change in δE until exciton saturation sets in at much higher pump powers. The behavior is typical in polariton lasers. The blueshift is caused by repulsive self-interaction of the exciton-polaritons and the resultant renormalization of the exciton self energy²⁴. From the blueshift, the exciton-polariton population N_{3D} may be estimated using $\delta E \approx 3.3\pi E_X^B a_B^3 N_{3D}$,⁶ where $E_X^B = 30$ meV is the X_A exciton binding energy and $a_B = 3.5$ nm is the exciton Bohr radius. We found $N_{3D} = 1.43 \times 10^{17} \text{ cm}^{-3}$ at threshold. This value is a factor of 7 larger than that estimated from the incident excitation energy, which could be due to a couple of reasons. The first is the spread of values of a_B for GaN quoted in the literature. Second, the exciton population introduces both phase space filling and a saturation of the oscillator strength, both resulting in a blueshift of the lower polariton energy. The formula quoted above is based on phase space filling only. Hence the exciton population calculated based on the total measured blueshift is higher than the actual exciton population.

With further increase of excitation density (by using an objective lens and spot size of ~ 10 μm) to $(10^2-10^3)E_{th1}$, the emission becomes strongly blueshifted and broadened (see

supplementary information), indicating exciton saturation and transition to the weak coupling regime⁸. A second distinct threshold was observed at $E_{\text{th2}} \approx 2700E_{\text{th1}} = 250 \mu\text{J}/\text{cm}^2$, which correspond to a population slightly higher than the Mott density and represents the onset of photon lasing. The integrated emission intensity over the entire range of excitation power density is shown in Fig. 2(c). The two distinct thresholds, three orders of magnitude apart in excitation density, are strong evidence of the very different origin of the nonlinear emissions. Polariton lasing results from stimulated scattering of polaritons into the quantum degenerate polariton states at $k_{\parallel} \sim 0$, without requiring population inversion. Photon lasing results from stimulated emission into the cavity modes upon population inversion in the electronic media.

To confirm the physical mechanism for the first nonlinear threshold, we measured the LP population distribution in k-space by angle-resolved photoluminescence. Figure 3 shows the spectra of angle-resolved PL between 0° and 27° at 300 K, both below (a) and above (b) threshold. There is no obvious energy-relaxation bottleneck at all excitation densities. Below threshold, emission intensities are comparable at different angles. Above threshold, the emission becomes sharply peaked at small angles, showing condensation in k-space. The number of polaritons per k_{\parallel} state is estimated from the PL intensity by taking into account the radiative lifetime of polaritons²⁵ and is shown in Fig. 3(c). As can be seen again that below threshold the distribution is random where as above threshold there is a sharp increase in the occupancy near $k_{\parallel} \sim 0$ states.

Coherence properties of the emission below and above E_{th1} were also studied and the measured data are shown in the supplementary document. The first order coherence was measured with a Michelson interferometer using pulsed excitation. Below threshold, the interference fringe contrast has a noise limited value of $\sim 2.5\%$ and it increased to a value of $\sim 32\%$

at threshold (92.5 nJ/cm^2). The second order coherence function in time domain was measured as a function of incident excitation energy by a Hanbury-Brown and Twiss type measurement system. Similar results as reported by Kasprzak et al²⁷ were obtained.

In conclusion, room temperature polariton lasing at record low threshold polariton densities was achieved in a vertical microcavity containing a single GaN nanowire. The threshold density was two orders of magnitude lower than reported values for GaN-based polariton lasers. Dynamic and coherence properties of the device all suggest that the low-threshold lasing results from stimulated scattering and accumulation of a quantum degenerate polariton population near the band minimum. In comparison, a second threshold corresponding to conventional photon lasing was also observed at a density 2700 times the polariton lasing threshold density. Reducing the lateral size of the microcavity would increase the photon-exciton coupling and further improve the optical qualities of the polariton laser. Our work represents a first step in developing a new generation of ultra-low power and ultra-compact, room-temperature photonic devices based on GaN nanowire polaritons.

The work was supported by KAUST under Grant N012509-00. L. Zhang acknowledges support by the Elizabeth Crosby Award through the NSF Advance Program.

References

1. C. Weisbuch *et al.*, *Phys. Rev. Lett.*, **69**, 3314 (1992).
2. G. Khitrova *et al.*, *Rev. Mod. Phys.*, **71**, 1591 (1999).
3. H. Deng, H. Haug, and Y. Yamamoto, *Rev. Mod. Phys.*, **82**, 1489 (2010).
4. A. Imamoglu *et al.*, *Phys. Rev. A*, **53**, 4250 (1996).
5. H. Deng *et al.*, *Proc. Nat. Acad. Sci. USA*, **100**, 15318 (2003).
6. S. Christopoulos *et al.*, *Phys. Rev. Lett.*, **98**, 126405 (2007).
7. S. Kéna-Cohen and S.R. Forrest, *Nature Photon*, **4**, 371 (2010).
8. D. Bajoni *et al.*, *Phys. Rev. Lett.*, **100**, 047401 (2008).
9. N. Antoine-Vincent *et al.*, *Phys. Rev. B*, **68**, 153313 (2003); R. Butté *et al.*, *Phys. Rev. B*, **73**, 033315 (2006).
10. B. Sermage and G. Fishman, *Phys. Rev. B*, **5107** (1981).
11. L. K. van Vugt *et al.*, *Phys. Rev. Lett.*, **97**, 1471401 (2006).
12. D. G. Lidzey *et al.*, *Nature*, **53**, 395 (1998).
13. G. Christmann *et al.* *Appl. Phys. Lett.*, **93**, 051102 (2008).
14. G. Christmann *et al.*, *Phys. Rev. B*, **77**, 085310 (2008).
15. T. Böttcher *et al.*, *Phys. Stat. Sol. (c)* **0**, 6 1846 (2003).
16. J. Schlager *et al.*, *J. Appl. Phys.*, **103**, 124309 (2008).
17. W. Guo *et al.*, *Appl. Phys. Lett.*, **98**, 183116(2011).
18. K.A. Bertness *et al.*, *J. Cryst. Growth*, **287** (2) 522– 527(2006).
19. C. Chéze *et al.*, *Nano Research*, **3** (7) 528– 536 (2010).
20. W. Guo *et al.*, *Nano lett.*, **11** (4), 1434 (2011); W. Guo *et al.*, *Nano Lett.*, **10** (9), 3355 (2010).
21. A. Cavallini *et al.*, *Nano lett.*, **17**(7), 2166 (2007).

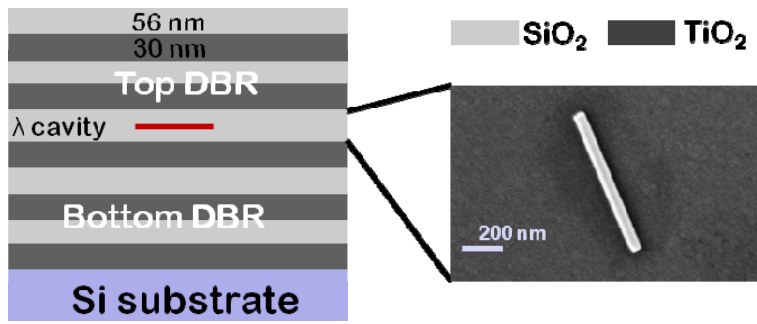
22. O. Mayrock, *Localization, Disorder, and Polarization Fields in Wide-Gap Semiconductor Quantum Wells*, Ph.D. Thesis, Humboldt-Universität zu Berlin, Berlin (2001).
23. F. Binet *et al.*, *Phys. Rev. B*, **60**, 4715 (1999).
24. N. Peyghambarian *et al.*, *Phys. Rev. Lett.*, **53**, 2433 (1984).
25. The occupation number ($N_{LP}(k_{||})$) is calculated from the intensity ($I_{LP}(k_{||})$) by using the formula, $I_{LP}(k_{||}) = \eta N_{LP}(k_{||}) |C(k_{||})|^2 M / \tau_C$, where η is the collection efficiency, $\tau_C / |C(k_{||})|^2$ is the radiative lifetime of the LPs and M is the number of transverse states subtended by the detection cone. (see H. Deng *et al.*, *Phys. Rev. Lett.*, **97**, 146402(2006).)
27. J. Kasprzak *et al.*, *Phys. Rev. Lett.*, **100**, 067402 (2008).

Figure Captions:

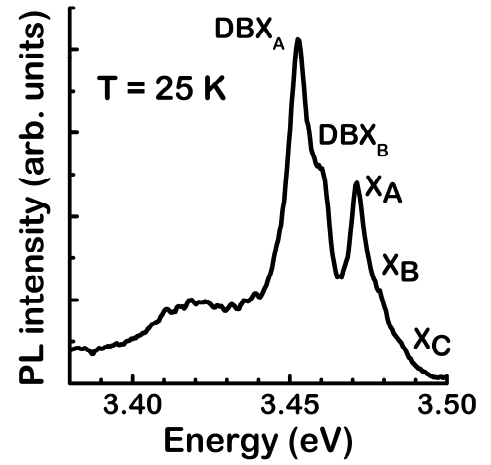
Figure 1 (a) Schematic representation of the dielectric microcavity with a single GaN nanowire of diameter 60 nm (inset) buried in the center of a λ -sized cavity; (b) photoluminescence spectrum from a single GaN nanowire measured at 25K showing free and bound exciton transitions; (c) angle-resolved photoluminescence measured at room temperature; (d) polariton dispersion curves obtained from the data of (c). The solid curves indicate the calculated polariton dispersion from a coupled harmonic oscillator model.

Figure 2 (a) Measured polariton emission intensity at 200K as a function of incident optical excitation energy showing strong non-linearity at threshold. The inset shows the emission spectra; (b) variation of the emission linewidth and peak energy corresponding to the data in (a); (c) variation of the emission intensity with excitation energy at 300K clearly showing the two thresholds for polariton and photon lasing. The insets show the corresponding emission spectra; (d) variation of linewidth and emission energy at 300K for polariton lasing.

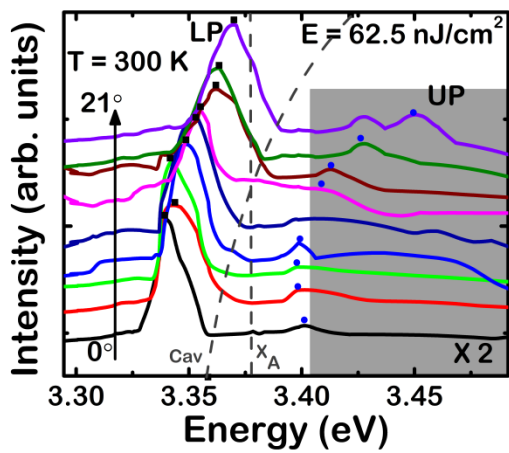
Figure 3 Angle resolved lower polariton luminescence spectra measured at 300K (a) below and (b) above the polariton lasing threshold; (c) polariton occupancy for different $k_{||}$ states deduced from the data of Figs. (a) and (b).



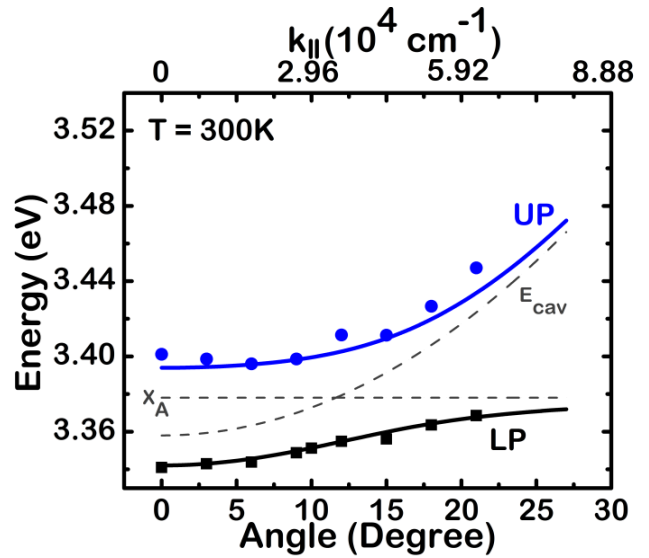
(a)



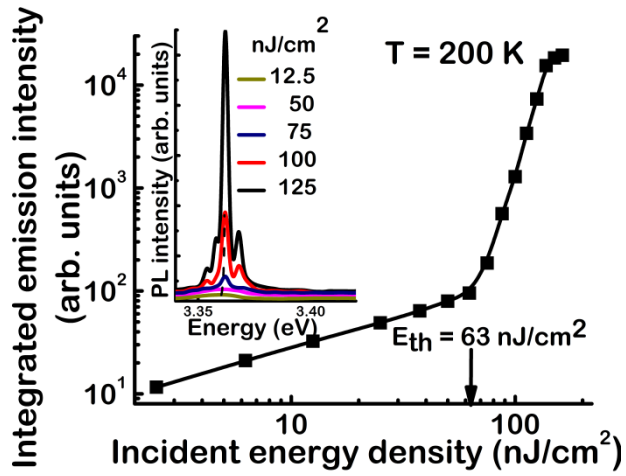
(b)



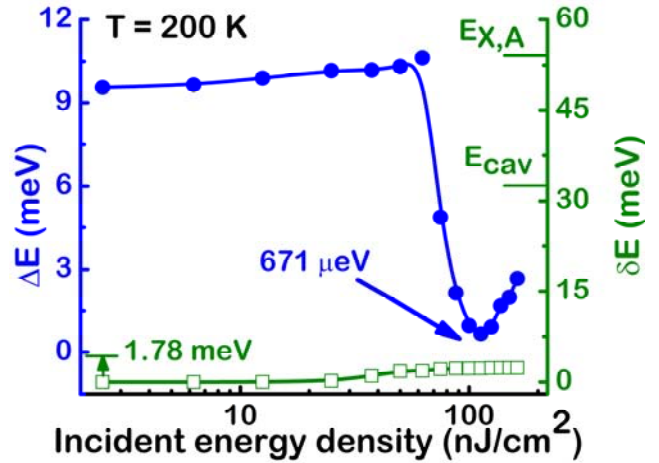
(c)



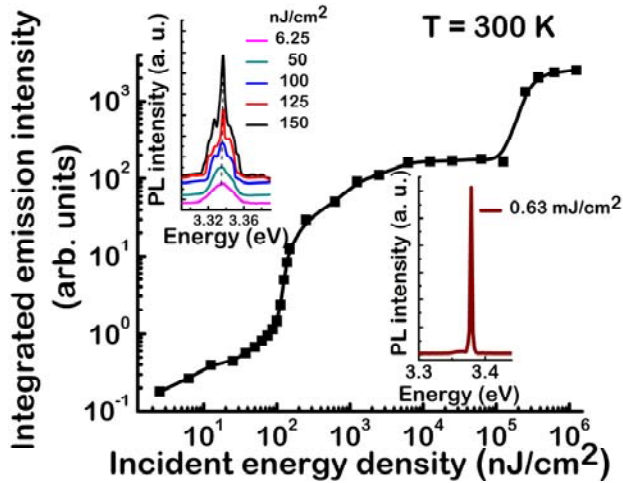
(d)



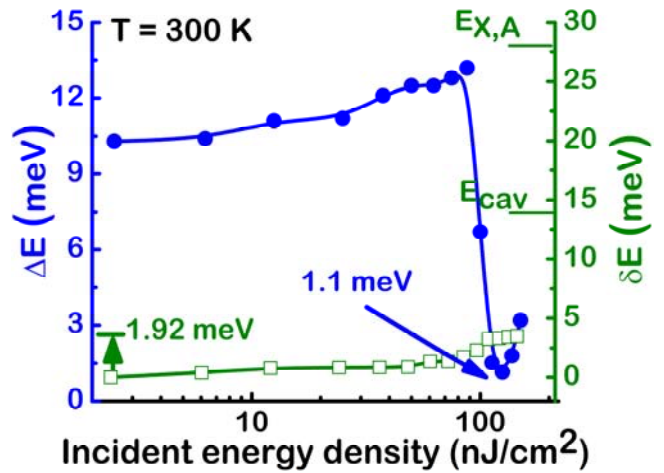
(a)



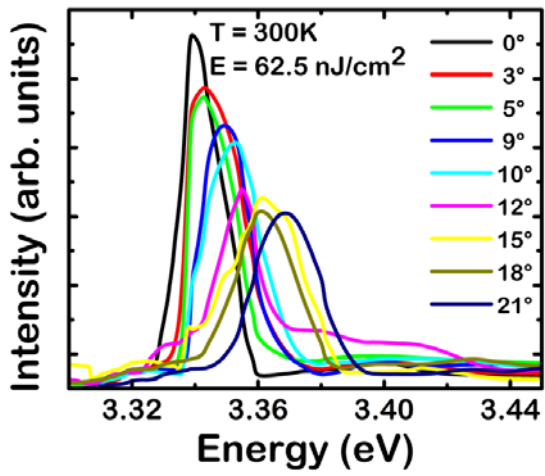
(b)



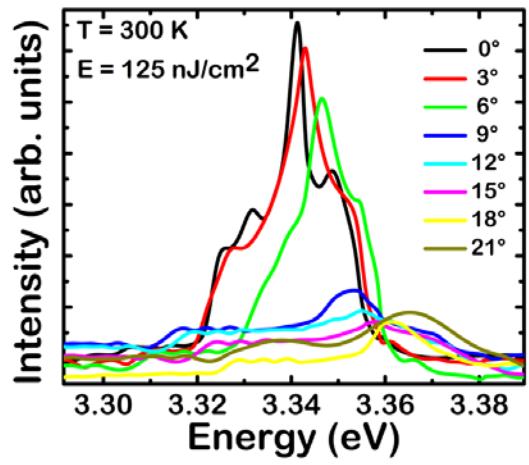
(c)



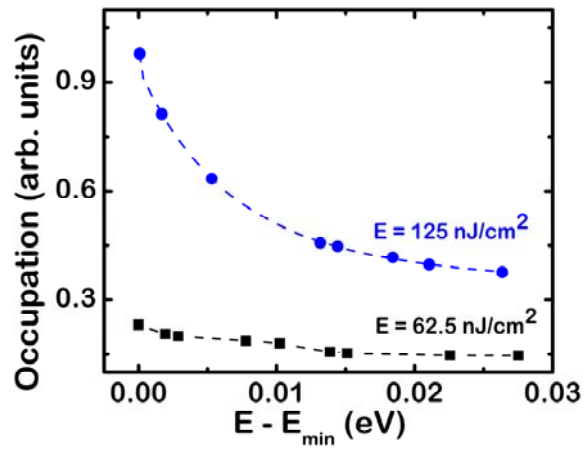
(d)



(a)



(b)



(c)